


## Article

# Chemical-Anatomical Characterization of Stems of Asparagaceae Species with Potential Use for Lignocellulosic Fibers and Biofuels

Agustín Maceda <sup>1</sup>, Marcos Soto-Hernández <sup>2</sup>  and Teresa Terrazas <sup>1,\*</sup> 

<sup>1</sup> Instituto de Biología, Universidad Nacional Autónoma de México, Mexico City 04510, Mexico

<sup>2</sup> Programa de Botánica, Colegio de Postgraduados, Montecillo 56230, Mexico

\* Correspondence: tterrazas@ib.unam.mx; Tel.: +52-55-5622-9116

**Abstract:** During the last decades, the possibility of using species resistant to droughts and extreme temperatures has been analyzed for use in the production of lignocellulosic materials and biofuels. Succulent species are considered to identify their potential use; however, little is known about Asparagaceae species. Therefore, this work aimed to characterize chemically-anatomically the stems of Asparagaceae species. Stems of 10 representative species of Asparagaceae were collected, and samples were divided into two. One part was processed to analyze the chemical composition, and the second to perform anatomical observations. The percentage of extractives and lignocellulose were quantified, and crystalline cellulose and syringyl/guaiacyl lignin were quantified by Fourier transform infrared spectroscopy. Anatomy was observed with epifluorescence microscopy. The results show that there were significant differences between the various species ( $p < 0.05$ ) in the percentages of extractives and lignocellulosic compounds. In addition, there were anatomical differences in fluorescence emission that correlated with the composition of the vascular tissue. Finally, through the characterization of cellulose fibers together with the proportion of syringyl and guaiacyl, it was obtained that various species of the Asparagaceae family have the potential for use in the production of lignocellulosic materials and the production of biofuels.

**Keywords:** Asparagaceae; lignocellulose; crystalline cellulose; syringyl/guaiacyl; anatomy



**Citation:** Maceda, A.; Soto-Hernández, M.; Terrazas, T. Chemical-Anatomical Characterization of Stems of Asparagaceae Species with Potential Use for Lignocellulosic Fibers and Biofuels. *Forests* **2022**, *13*, 1853. <https://doi.org/10.3390/f13111853>

Academic Editors: Vicelina Sousa, Helena Pereira, Teresa Quilhó and Isabel Miranda

Received: 3 October 2022

Accepted: 3 November 2022

Published: 6 November 2022

**Publisher's Note:** MDPI stays neutral with regard to jurisdictional claims in published maps and institutional affiliations.



**Copyright:** © 2022 by the authors. Licensee MDPI, Basel, Switzerland. This article is an open access article distributed under the terms and conditions of the Creative Commons Attribution (CC BY) license (<https://creativecommons.org/licenses/by/4.0/>).

## 1. Introduction

Asparagaceae is one of the most important families in Mexico due to its biological, economic, and cultural importance [1]. Several species are used in the production of fibers, intoxicating drinks, food preparation, and the consumption of plant parts (flower, stem, and leaf) [2]. Asparagaceae has several subfamilies, including Agavoideae with *Agave*, *Furcraea*, *Manfreda*, and *Polianthes*; Yuccoideae including *Yucca*, *Hesperaloe*, and *Hesperoyucca* [3], and the subfamily Nolinoideae that includes the genera *Beaucarnea* and *Nolina* [4]. Most of the species of Agavoideae and Nolinoideae are distributed in arid and semiarid, and warm temperate regions of North and Central America [3] and in other parts of the world naturally or introduced. Several species of *Agave* have been used and studied the most because ethanol is produced in the form of intoxicating beverages such as *mezcal* and *tequila* [5].

In recent years, mainly the fibers and bagasse waste of several agave species, mainly *A. tequilana* [6,7], *A. angustifolia* [8], and *A. salmiana* [9] have been studied because a large amount of waste is produced annually from the production of *tequila* and *mezcal*. In addition, the subfamilies Agavoideae and Nolinoideae present acid metabolism of the crassulacean (CAM), which is considered raw material for the production of biofuel [10,11]. Furthermore, these species are part of the second generation of plants focused on biofuels. They are not part of the plants essential for human consumption [12], and they tolerate drought conditions and high temperatures [13].

Other species within the group of the second generation are cacti, such as *Opuntia* spp. [14], which also withstand extreme drought conditions and have CAM metabolism [15]. However, except for some genera such as *Opuntia* spp. and *Selenicereus* spp. [16,17], the other cacti species have slow vegetative development or very small sizes [18], so they could not be profitable in their use as biofuels or production of paper, while in species of the genus *Agave* growth and yield are higher [19].

However, even though many species of Asparagaceae exist in Mexico, there is not much information on the composition of the main lignocellulosic structural components, the anatomical distribution, or the potential use for farmers to cultivate and protect the plants in their natural environment [1]. Therefore, the objectives were to characterize the different Asparagaceae species with the extractives and lignocellulosic percentages, obtain crystallinity indexes, syringyl/guaiacyl (S/G) lignin ratio, and the anatomical distribution, with which it will be possible to identify the potential use of the different species as biofuels or in the paper industry, in addition to the possible biological implications.

## 2. Materials and Methods

### 2.1. Plant Materials and Extractives

Healthy adult plants were donated from the *Universidad Nacional Autónoma de México* (UNAM) Botanical Garden collection (Table 1), located at 19°18'44" N, 99°11'46" O and 2320 m a. s. l. The climate of the area is temperate, with rain in summer, with the rainy season from June to October, and the dry season from November to May. It has an average annual temperature of 15.6 °C and a rainfall of 833 mm. The plants were collected in their natural populations and grew in the garden. The leaves and stems of the ten species were cut, and only the stem was selected for the study. Stem samples were cut into pieces and dried in an oven for two weeks at 70 °C. Subsequently, the samples were ground (40–60 mesh size, Cyclone Sample Mill, (UDY Corporation, Fort Collins, CO, USA) until a particle size of 0.4 mm was obtained.

**Table 1.** Asparagaceae Species.

Species	Type of Stem	Life Forms	Size Category	Natural Distribution
<i>Agave attenuata</i> Salm-Dyck	Fibrous	Herbaceous	Medium	Mexico
<i>Agave celsii</i> Hook.	Fibrous	Herbaceous	Medium	Mexico
<i>Agave convallis</i> Trel.	Fibrous	Herbaceous	Medium	Mexico
<i>Agave striata</i> Zucc.	Fibrous	Herbaceous	Medium	Mexico
<i>Beaucarnea gracilis</i> Lem.	Fibrous	Arborescent	Tall	Mexico
<i>Furcraea longeva</i> Karw. & Zucc.	Fibrous	Arborescent	Tall	Mexico
<i>Nolina excelsa</i> García-Mend. & E. Solano	Fibrous	Arborescent	Tall	Mexico
<i>Yucca filifera</i> Chabaud	Fibrous	Arborescent	Tall	Mexico
<i>Yucca gigantea</i> Lem.	Fibrous	Arborescent	Tall	Mexico, Guatemala
<i>Yucca periculosa</i> Baker	Fibrous	Arborescent	Tall	Mexico

The samples were analyzed in triplicate based on the TAPPI T-222 om-02 standard and based on the method proposed by Maceda et al. [20,21]. From each ground sample, 2 g were taken, which were placed in filter paper cartridges to carry out successive extractions for six hours in a Soxhlet with ethanol-benzene (1:2 v/v) and subsequently in ethanol (96%). After each extraction, the cartridges were allowed to dry for 24 h at 70 °C to record their constant weight.

Subsequently, the cartridges were discarded, and the samples were kept in a reflux system for 1 h in water at 90 °C. The samples were filtered through a medium pore Büchner filter and dried at 70 °C for 24 h to record constant dry weight. The formula used was the following:

$$\text{Total extractives (\%)} = [(A + B + C) / W_0] \times 100$$

where *A* is the weight lost (g) after extraction with ethanol:benzene, *B* is the weight lost (g) after extraction with ethanol (96%), *C* is the weight lost (g) after extraction with water at

90 °C, and  $W_0$  is the initial weight of each sample. The percentage of extractive-free lignocellulose was obtained by subtracting from 100% the initial weight of the total percentage of extractives.

## 2.2. Lignocellulosic Purification

**Klason lignin.** From the extractive-free lignocellulose of each species, 0.2 g were taken, and 15 mL of concentrated sulfuric acid (72%) was added at a temperature of 2 °C. The mixture was kept under constant stirring and at room temperature (18 °C) for 2 h. Then, 560 mL of distilled water was added, and the mixture was refluxed and boiled for 4 h. The samples were filtered through a fine-pore Büchner filter and dried at 105 °C for 24 h to record constant dry weight. Lignin was quantified as follows:

$$\text{Klason lignin (\%)} = (W_L / W_W) \times 100$$

where  $W_L$  is the obtained weight of lignin (g), and  $W_W$  is the extractives-free lignocellulose (g).

**Cellulose.** From the extractive-free lignocellulose, 0.2 g were taken to purify the cellulose using the Kùshner-Höffer method [21]. Twenty-five mL of  $\text{HNO}_3$ /ethanol (1:4 v/v) were added to each sample and kept in a reflux system, and boiled for one hour. The sample was allowed to decant to discard the  $\text{HNO}_3$ /ethanol solution, and another 25 mL was added again. This cycle was repeated three more times, and in the last cycle, 25 mL of an aqueous solution of KOH at 1% was added and kept for 30 min at reflux and boiling to finally filter the sample through a fine-pore Büchner filter. The sample was left to dry at 70 °C for 12 h to record the constant dry weight and obtain the percentage of cellulose based on the following formula:

$$\text{Cellulose (\%)} = (W_C / W_W) \times 100$$

where  $W_C$  is the obtained weight of cellulose(g), and  $W_W$  is the extractives-free lignocellulose (g).

**Hemicellulose.** The purification was carried out based on the methodology proposed by Li. et al. [22]. From the extractive-free lignocellulose, 0.5 g were taken and placed in a reflux system with 10 mL of water for 3 h (solid-to-liquid ratio 1:20 g/mL). The system was cooled to room temperature and filtered. The filtrate was concentrated at 1.25 mL and purified into 3.75 mL of ethanol (95%) with stirring. The mixture was held for 1 h without stirring, and the hemicellulose precipitated. In order to obtain the dry weight ( $H_0$ ), the sample was centrifuged at  $4500 \times g$  for 4 min, and then lyophilized. The residue insoluble in water was dried at 60 °C for 16 h, then successive extractions were performed with different concentrations of KOH (0.6, 1.0, 1.5, 2.0, and 2.5%) in a ratio of 1:20 (g/mL) at 75 °C for 3 h in each extraction. In the last concentration of 2.5% KOH, ethanol (99.7%) was added in a ratio of 2:3. The five mixtures were filtered and acidified to pH 5.5 with glacial acetic acid and concentrated to 1.25 mL. The mixtures were poured into 3.75 mL of ethanol (95%) with constant stirring. The mixtures were kept for 1 h and finally were centrifuged ( $4500 \times g$  for 4 min) and lyophilized. The constant dry weight was recorded in each extraction stage ( $H_{0.6}$ ,  $H_{1.0}$ ,  $H_{1.5}$ ,  $H_{2.0}$ ,  $H_{2.5}$ ), and the percentage of cellulose was obtained with the following formula:

$$\text{Hemicellulose (\%)} = (W_H / W_W) \times 100$$

where  $W_H$  is the sum of  $H_{0.6}$  to  $H_{2.5}$  and  $W_W$  is the extractive-free lignocellulose (g).

## 2.3. Fourier Transform Infrared Spectroscopy Analysis

**Lignin analysis.** The ratio of syringyl/guaiacyl monomers (S/G) was obtained by Fourier transform infrared spectroscopy (FTIR) analysis. Klason lignin samples were kept dry until analyzed by FTIR (30 scans with a resolution of  $4 \text{ cm}^{-1}$ , 15 s per repeat). Three FTIR readings (Agilent Cary 630 FTIR) were made from each sample, and then the

baseline correction was performed to separate the peaks of the fingerprints (wavelength of  $800\text{--}1800\text{ cm}^{-1}$ ) [23] in the MicroLab PC program (Agilent Technologies). The peaks of  $1269\text{ to }1272\text{ cm}^{-1}$  and  $1328\text{ to }1330\text{ cm}^{-1}$  were used to quantify the proportion of guaiacyl (G) and syringyl (S), respectively [24]. The value of each peak was obtained by drawing a line connecting the lowest values and a similar line for the highest values of each peak. A vertical line was drawn from the base of the X-axis to the highest part of the peak. The portion of the line between the top and the base is the value of each peak, so the S/G ratio was calculated by dividing the values of each peak [24].

**Cellulose analysis.** The proportion of crystalline cellulose was obtained by analyzing the dried samples with FTIR [21]. From each sample and doing the analyzes in triplicate, a small portion of the sample was placed in the FTIR Spectrometer (Agilent Cary 630 FTIR), and the spectrum was obtained in a range of  $400\text{--}650\text{ cm}^{-1}$  (30 scans with a resolution of  $4\text{ cm}^{-1}$ , 15 s per repeat). Samples were converted from transmittance to absorbance, and spectra were averaged using the Resolution Pro FTIR Software program (Agilent Technologies, Santa Clara, CA, United States).

The crystallinity indices used were: Total crystallinity index (TCI) proposed by Nelson and O'Connor [25] or also called the crystallinity ratio [26,27]. The lateral order index (LOI) [25,27] or second proportion of crystallinity [26]; and hydrogen bonding intensity (HBI) [28]. TCI was calculated with the ratio between the absorption intensity of the peaks  $1370\text{ cm}^{-1}$  and  $2900\text{ cm}^{-1}$  [27], LOI was calculated from the ratio between the absorption intensity of the peaks  $1430\text{ cm}^{-1}$  and  $893\text{ cm}^{-1}$  [26], while HBI was calculated with the ratio between  $3350\text{ cm}^{-1}$  and  $1315\text{ cm}^{-1}$  [28].

#### 2.4. Statistical Analysis

The data obtained from the percentages of extractives and lignocellulosic components were analyzed with the non-parametric Kruskal-Wallis test and Dunn's post hoc analysis since the values did not present normality based on the results of Kolmogorov-Smirnov and Shapiro-Wilk, even when they were transformed with the square root of the arc sine. In addition, a multivariate principal component analysis was performed to separate the groups based on the values of the structural components.

#### 2.5. Lignocellulosic Anatomical Distribution

Stem fragments were saved from each sample and were fixed, embedded, and cut based on the procedures of Arias and Terrazas [29] for succulent hardwood species. The transverse sections were stained with acridine orange and calcofluor [30] to observe the distribution of cellulose and lignin in the stem, in addition to comparing the anatomical results with the chemical ones.

### 3. Results

#### 3.1. Extractives and Lignocellulosic Structural Compounds

The Asparagaceae species had significant differences between species (Table 2) in the variables of extractives and lignocellulosic components. The percentages of extractives were heterogeneous between the species of the same genus; however, the differences occurred mainly between *Agave* and *Yucca-Nolina*. In Tables 3 and 4, the means and standard deviation of the extractives are presented, and the different superscript capital letters show the species that are significantly different. In the ethanol extractives, *A. striata* had the lowest percentage and was significantly different from *Y. gigantea*, which had the highest percentage (Table 3). In hot water extractives, a similar situation was shown; *A. convallis* had the highest percentage, while *N. excelsa* and *Y. periculosa* had the lowest percentage. In the ethanol:benzene extractives, the statistical differences were presented between *N. excelsa*, with the lowest percentage, and *F. longavea*, with the highest percentage. The species with the highest content of extractives and the lowest content of lignified tissue were *A. convallis* and *Y. gigantea*. On the contrary, the species with the lowest content of extractives and the highest amount of lignified tissue were *N. excelsa* and *Y. periculosa*.

**Table 2.** Kruskal-Wallis analysis for the lignocellulosic and extractives variables.

Variables	$\chi$ -Square	Df	Significance
Ethanol-benzene	21.16344	9	0.01194
Ethanol 96%	22.17698	9	0.00833
Water 90 °C	24.08278	9	0.00417
Total extractives	26.28172	9	0.00184
Extractive-free lignocellulose	26.28172	9	0.00184
Lignin	20.94839	9	0.01288
Cellulose	26.64249	9	0.00160
Hemicelluloses	24.54409	9	0.00352

**Table 3.** Extractives percentage from the 10 Asparagaceae species.

Species	Extractive Compounds (%)				Extractive-Free Lignocellulose (%)
	Ethanol–Benzene	Ethanol 96%	Water 90 °C	Total Extractives	
<i>Agave attenuata</i>	7.5 ± 1.8 <sup>AB</sup>	9.9 ± 1.1 <sup>AB</sup>	4.7 ± 1.1 <sup>AB</sup>	22.0 ± 1.8 <sup>ABC</sup>	78.0 ± 1.8 <sup>ABC</sup>
<i>Agave celsii</i>	6.9 ± 1.8 <sup>AB</sup>	6.5 ± 1.1 <sup>AB</sup>	3.9 ± 0.8 <sup>AB</sup>	17.4 ± 0.8 <sup>ABC</sup>	82.6 ± 0.8 <sup>ABC</sup>
<i>Agave convallis</i>	9.4 ± 1.9 <sup>AB</sup>	6.4 ± 1.2 <sup>AB</sup>	10.2 ± 1.5 <sup>B</sup>	26.0 ± 0.5 <sup>C</sup>	74.0 ± 0.5 <sup>A</sup>
<i>Agave striata</i>	7.6 ± 1.6 <sup>AB</sup>	4.6 ± 0.7 <sup>A</sup>	3.0 ± 0.7 <sup>AB</sup>	15.3 ± 2.5 <sup>ABC</sup>	84.7 ± 2.5 <sup>ABC</sup>
<i>Beaucarnea gracilis</i>	5.9 ± 0.5 <sup>AB</sup>	8.3 ± 1.9 <sup>AB</sup>	5.3 ± 0.5 <sup>AB</sup>	19.5 ± 1.8 <sup>ABC</sup>	80.5 ± 1.8 <sup>ABC</sup>
<i>Furcraea longaevea</i>	9.7 ± 0.6 <sup>B</sup>	6.9 ± 0.7 <sup>AB</sup>	3.7 ± 0.7 <sup>AB</sup>	20.2 ± 0.8 <sup>ABC</sup>	79.8 ± 0.8 <sup>ABC</sup>
<i>Nolina excelsa</i>	4.5 ± 0.9 <sup>A</sup>	5.1 ± 0.6 <sup>AB</sup>	1.7 ± 0.6 <sup>A</sup>	11.3 ± 1.1 <sup>A</sup>	88.7 ± 1.1 <sup>C</sup>
<i>Yucca filifera</i>	9.6 ± 0.2 <sup>AB</sup>	6.2 ± 1.1 <sup>AB</sup>	3.2 ± 0.2 <sup>AB</sup>	18.9 ± 0.9 <sup>ABC</sup>	81.1 ± 0.9 <sup>ABC</sup>
<i>Yucca gigantea</i>	8.4 ± 1.1 <sup>AB</sup>	11.9 ± 1.2 <sup>B</sup>	3.8 ± 0.9 <sup>AB</sup>	24.1 ± 2.2 <sup>BC</sup>	75.9 ± 2.2 <sup>AB</sup>
<i>Yucca periculosa</i>	6.1 ± 1.8 <sup>AB</sup>	4.9 ± 1.0 <sup>AB</sup>	1.8 ± 0.6 <sup>A</sup>	12.9 ± 2.5 <sup>AB</sup>	87.1 ± 2.5 <sup>BC</sup>

Different letters in each column indicate significant differences ( $p < 0.05$ ). Mean ± standard deviation (SD).

**Table 4.** Lignin, cellulose, and hemicellulose percentage of dry biomass of Asparagaceae species.

Species	Lignin (%)	Cellulose (%)	Hemicellulose (%)
<i>Agave attenuata</i>	20.4 ± 2.7 <sup>AB</sup>	35.4 ± 0.8 <sup>ABC</sup>	22.1 ± 1.6 <sup>ABC</sup>
<i>Agave celsii</i>	23.8 ± 0.9 <sup>AB</sup>	31.6 ± 0.8 <sup>A</sup>	27.1 ± 2.3 <sup>BC</sup>
<i>Agave convallis</i>	18.2 ± 1.8 <sup>AB</sup>	34.9 ± 1.4 <sup>AB</sup>	20.9 ± 1.6 <sup>ABC</sup>
<i>Agave striata</i>	24.2 ± 6.1 <sup>AB</sup>	37.1 ± 1.9 <sup>ABC</sup>	23.4 ± 5.9 <sup>ABC</sup>
<i>Beaucarnea gracilis</i>	20.2 ± 1.1 <sup>AB</sup>	38.1 ± 1.7 <sup>ABC</sup>	22.3 ± 2.8 <sup>ABC</sup>
<i>Furcraea longaevea</i>	26.3 ± 0.8 <sup>B</sup>	37.3 ± 0.9 <sup>ABC</sup>	16.2 ± 2.4 <sup>ABC</sup>
<i>Nolina excelsa</i>	24.5 ± 3.2 <sup>AB</sup>	52.2 ± 2.1 <sup>C</sup>	12.0 ± 4.1 <sup>AB</sup>
<i>Yucca filifera</i>	11.4 ± 1.1 <sup>A</sup>	38.9 ± 1.2 <sup>ABC</sup>	30.7 ± 0.9 <sup>C</sup>
<i>Yucca gigantea</i>	24.9 ± 1.7 <sup>AB</sup>	45.3 ± 1.8 <sup>BC</sup>	5.7 ± 1.5 <sup>A</sup>
<i>Yucca periculosa</i>	24.5 ± 0.5 <sup>AB</sup>	41.6 ± 1.8 <sup>ABC</sup>	21.0 ± 2.3 <sup>ABC</sup>

Different letters in each column indicate significant differences ( $p < 0.05$ ). Mean ± standard deviation (SD).

The percentages of lignocellulosic components had significant differences in the percentages of lignin between *Y. filifera* and *F. longaevea* (Table 4). In cellulose, the species that had the lowest percentage were *A. celsii* and *A. convallis*, and *N. excelsa* was the species with the highest percentage. Finally, in the hemicelluloses, *Y. gigantea* presented the least quantity and *Y. filifera* the largest.

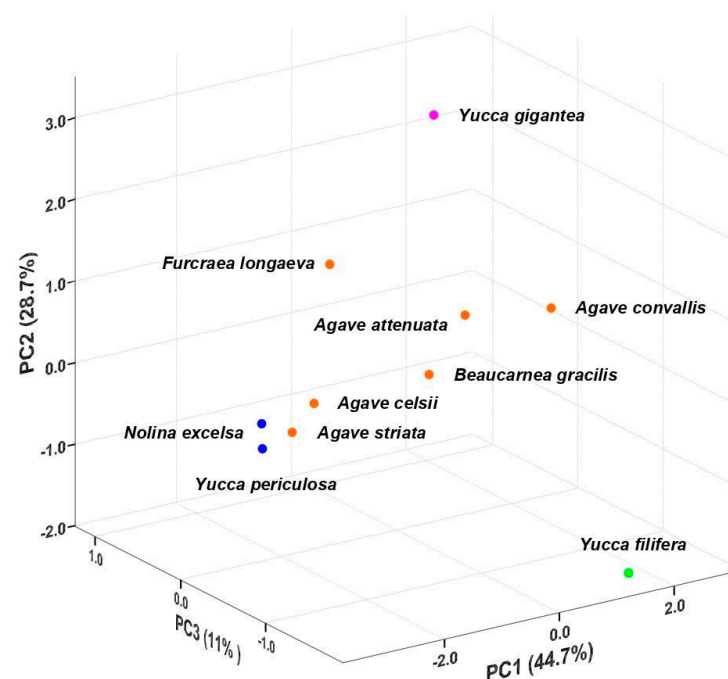
In the Principal Component (PC) analysis, the first two PCs had eigenvalues above 1, while PC3 was less than 1; however, PC3 was considered in the analysis due that it explained 11% of the variance, so the three PCs explained 84.5% of the total variation (Table 5). In each PC, the highest negative or positive values were those that influenced the separation of each species, as shown in Figure 1. For PC1, the variables that determined the separation of the different groups were hot water extractives and extractive-free lignocellulose. In PC2, the determinant variables of the variation were hemicelluloses and ethanol extractives, while in PC3 was the cellulose percentage (Table 5).



**Table 5.** Vectors, eigenvalues, and cumulative proportion of the variation are explained by each variable.

Variables	PC1	PC2	PC3
Ethanol-Benzene	0.439	0.058	0.013
Ethanol	0.194	<b>0.553</b>	−0.169
Water	<b>0.453 *</b>	0.096	0.125
Extractive-free lignocellulose	− <b>0.492</b>	−0.346	0.015
Cellulose	−0.327	0.302	<b>0.788</b>
Lignin	−0.410	0.272	−0.578
Hemicellulose	0.216	− <b>0.630</b>	−0.008
Eigenvalue	3.127	2.011	0.771
Variance (%)	44.7	28.7	11.0
Accumulative variance (%)	44.7	73.4	<b>84.4</b>

\* The highest values are in bold on each PC.

**Figure 1.** The three-dimension plot of the principal components from Asparagaceae stems. Blue points: group 1, green point: group 2, pink point: group 3, brown point: group 4.

When plotting the species based on the first three PCs and the variables that influenced each PC (Figure 1), the species were separated into four groups. The first group (blue points) included the species of *N. excelsa* and *Y. periculosa*, which were the species with the lowest content of hot water extractives and higher extractive–free lignocellulose content. The second group (green point), represented by *Y. filifera* had the highest percentage of hemicelluloses. The third group (pink point), conformed by *Y. gigantea* was separated from the other Yuccas and the other species because they had lower percentages of hemicelluloses, but it was one of the species with the highest percentage of cellulose and percentage of total extractives. In the fourth group (orange points), the remaining species that belong to *Agave*, *F. longaeve*, and *B. gracilis* were clustered (Figure 1).

### 3.2. Cellulose Crystallinity

In the cellulose spectra (Figure 2) and Table 6, the main cellulose peaks are observed. In order to determine the purity of the cellulose, the absence of xylans and hemicellulose was obtained by not detecting the peak at  $1735\text{ cm}^{-1}$ . Lignin was not detected with the peaks  $1595\text{ cm}^{-1}$ ,  $1512\text{ cm}^{-1}$ , and  $1463\text{ cm}^{-1}$ . Only weak lignin signals were observed in *A.*

*striata* and *Y. periculosa*. In addition, the absence of hemicellulose was observed without the presence of the  $1269\text{ cm}^{-1}$  peak, except for *A. celsii*, which had a weak peak.

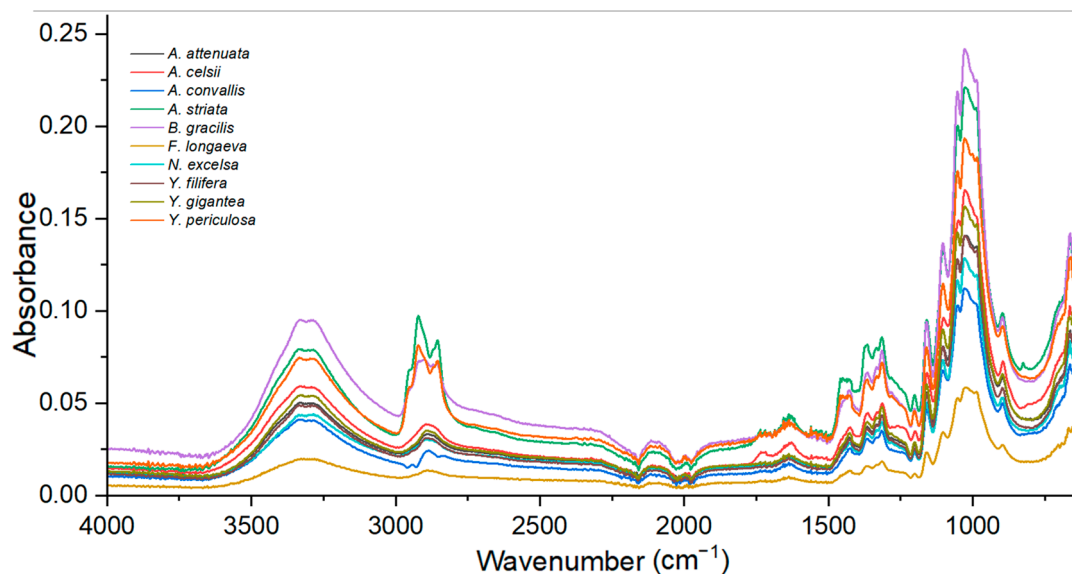


**Figure 2.** Cellulose FTIR spectra of Asparagaceae species.

**Table 6.** Cellulose peaks of Asparagaceae species.

Wavenumber ( $\text{cm}^{-1}$ )	Assignments
3000–3600	OH stretching
2900	CH stretching
1430	CH <sub>2</sub> symmetric bending (crystalline and amorphous cellulose)
1370	C-H and C-O bending vibration bonds
1336	C-O-H in-plane bending (amorphous cellulose)
1315	CH <sub>2</sub> wagging vibration (crystalline cellulose)
1163	C-O-C asymmetrical stretching
893	Out-of-plane asymmetrical stretching of cellulose ring
670	C-O-H out-of-plane stretching

In the crystallinity indexes (Table 7), the TCI values showed that most of the species had values above one because they had a higher percentage of crystalline cellulose, except *A. striata*, *B. gracilis*, and *Y. periculosa*, which presented a higher percentage of amorphous cellulose. In LOI, the species that had the highest value was *A. striata*, while the species that had the lowest value was *F. longaevea*, which had the highest value in TCI. In HBI, similarly, *A. striata* had the lowest value, while *B. gracilis* had the highest value.

**Table 7.** Crystallinity indexes of Asparagaceae species.

Species	TCI (A1370/A2900)	LOI (A1430/A893)	HBI (A3400/A1315)
<i>Agave attenuata</i>	$1.12 \pm 0.01$	$0.49 \pm 0.01$	$1.16 \pm 0.02$
<i>Agave celsii</i>	$1.15 \pm 0.05$	$0.49 \pm 0.03$	$1.18 \pm 0.09$
<i>Agave convallis</i>	$1.27 \pm 0.03$	$0.56 \pm 0.28$	$1.17 \pm 0.08$
<i>Agave striata</i>	$0.85 \pm 0.17$	$0.64 \pm 0.03$	$0.92 \pm 0.12$
<i>Beaucarnea gracilis</i>	$0.9 \pm 0.01$	$0.59 \pm 0.01$	$1.21 \pm 0.02$
<i>Furcraea longaevea</i>	$1.18 \pm 0.05$	$0.47 \pm 0.02$	$1.09 \pm 0.04$
<i>Nolina excelsa</i>	$1.09 \pm 0.1$	$0.54 \pm 0.02$	$1.09 \pm 0.01$
<i>Yucca filifera</i>	$1.16 \pm 0.02$	$0.52 \pm 0.01$	$1.11 \pm 0.02$
<i>Yucca gigantea</i>	$1.15 \pm 0.03$	$0.51 \pm 0.01$	$1.11 \pm 0.02$
<i>Yucca periculosa</i>	$0.78 \pm 0.05$	$0.59 \pm 0.02$	$1.03 \pm 0.05$

Mean  $\pm$  standard deviation (SD).

### 3.3. Lignin S/G Ratio

Figure 3 shows the FTIR spectra for the 10 species of Asparagaceae. Representative peaks of lignin were  $1501\text{ cm}^{-1}$  which showed the C=C aromatic ring vibration of syringyl and guaiacyl monomers. The  $1325\text{ cm}^{-1}$  peak reflected the breathing of the ring of syringyl in addition to C-O stretching. The  $1271\text{ cm}^{-1}$  and  $1225\text{ cm}^{-1}$  peaks reflected the symmetric vibration of C-O and the glucopyranose cycle of guaiacyl and syringyl, respectively. The  $1030\text{ cm}^{-1}$  peak reflected the C-H in-plane deformation of guaiacyl and C-O deformation in primary alcohol; finally, the  $913\text{ cm}^{-1}$  peaks showed the =CH out-of-plane deformation in the aromatic ring of syringyl and guaiacyl monomers (Figure 3).

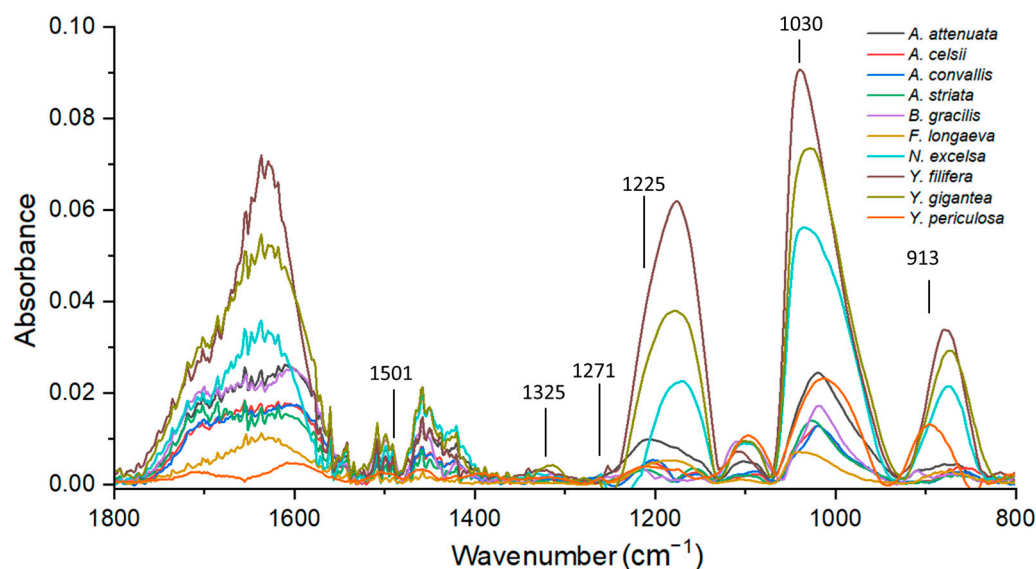


**Figure 3.** FTIR spectra of the lignin fingerprint of the Asparagaceae species.

With the peaks  $1325$  and  $1271\text{ cm}^{-1}$  the S/G ratio was calculated (Table 8). The species with the lowest proportion of S/G was *A. attenuata* because it had a higher percentage of guaiacyl in its structure, while in the genus *Yucca*, the three species presented high values of syringyl, for which the proportion of S/G was in the range of 2.8 to 3.9. The other species had similar proportions, so the syringyl monomer prevailed except in *A. convallis*.

**Table 8.** Percentages of syringyl and guaiacyl, and S/G ratio of Asparagaceae species.

Species	Guaiacyl (%)	Syringyl (%)	S/G Ratio
<i>Agave attenuata</i>	63.1	36.9	0.6
<i>Agave celsii</i>	47.0	53.0	1.1
<i>Agave convallis</i>	52.0	48.0	0.9
<i>Agave striata</i>	44.0	56.0	1.3
<i>Beaucarnea gracilis</i>	42.3	57.7	1.4
<i>Furcraea longaevea</i>	39.1	60.9	1.6
<i>Nolina excelsa</i>	49.0	51.0	1.0
<i>Yucca filifera</i>	26.1	73.9	2.8
<i>Yucca gigantea</i>	23.0	77.0	3.3
<i>Yucca periculosa</i>	20.5	79.5	3.9

### 3.4. Anatomical Distribution

The species of Asparagaceae studied showed the same type of vascular tissue, with closed vascular bundles forming isolated patches or two or more patches joined through lignified parenchyma. In the vascular bundle, the presence of tracheary elements with mainly reticular type of secondary wall thickenings was observed, with completely lignified fibers and non-lignified phloem with contents inside with fluorescence emission in bluish



tones (Figure 4). In most species, patches of non-lignified parenchyma were observed on the edges of the stem, while in the center, the parenchyma was completely lignified. In the species *A. attenuata* and *A. convallis*, the fluorescence tones of the tracheary elements and fibers predominated in yellow-green tones, while in the *Yucca* species, the fluorescence emission was observed in green to bluish-green tones. In all species, the presence of crystals was observed, mainly raphides and prisms. Cellulose fluoresced in bluish tones but differed from lignin due to the intensity of fluorescence emission since the cellulose had lower intensity compared to lignin.

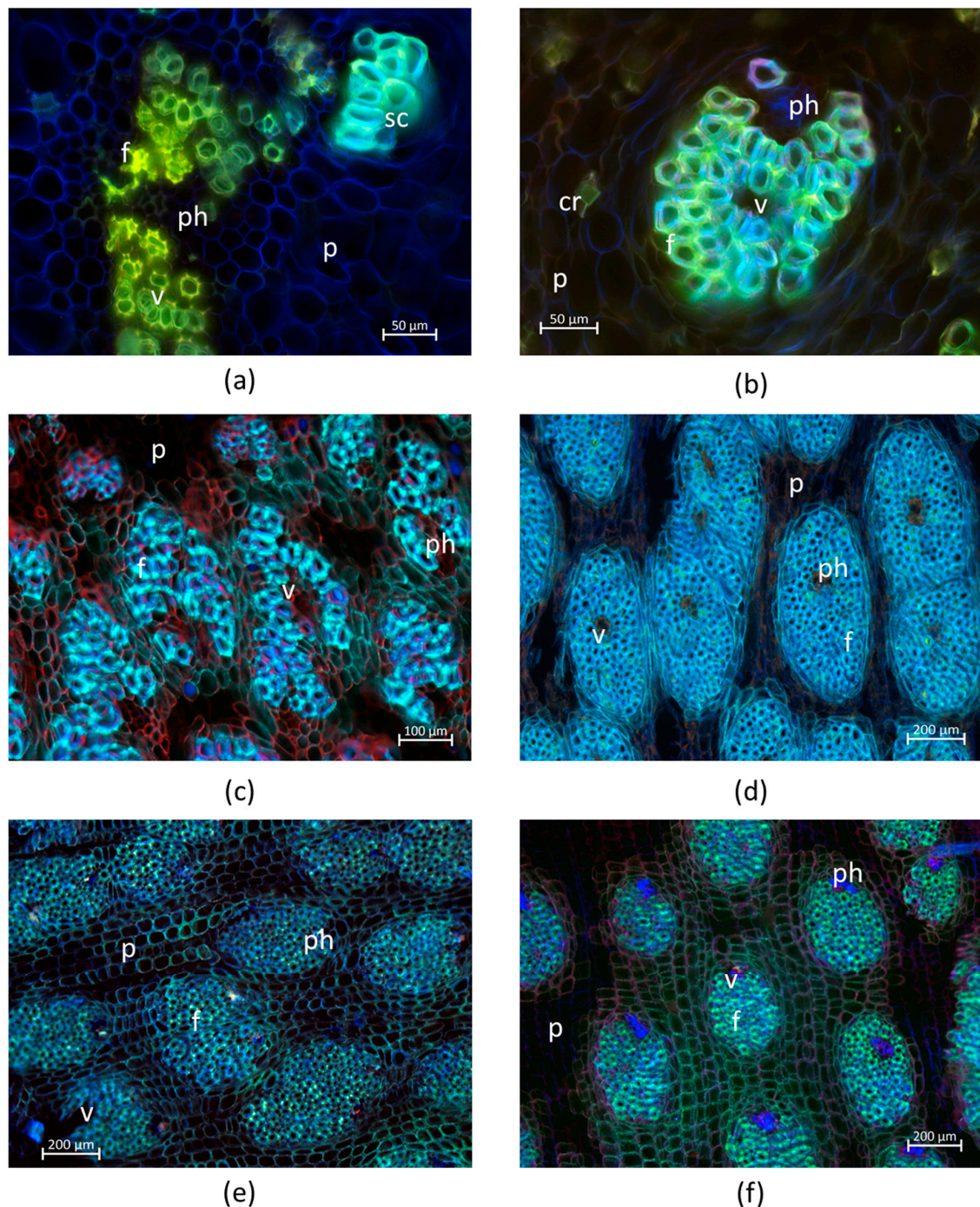


**Figure 4.** Fluorescence images from representative Asparagaceae species. (a) *A. attenuata*. (b) *A. convallis*. (c) *B. gracilis*. (d) *N. excelsa*. (e) *Y. gigantea*. (f) *Y. periculosa*. f: fiber, v: vessel, p: parenchyma, ph: phloem, cr: crystal.

#### 4. Discussion

The Asparagaceae family presented heterogeneity in the percentages of the structural components that allow its grouping based on the values of extractive compounds, hemicellulose, and cellulose. In addition, the presence of high percentages of cellulose, a majority proportion of crystalline cellulose, and the presence of S/G ratios greater than one make it possible to use in biofuels and cellulosic compounds.

##### 4.1. Extractives and Lignocellulose

Asparagaceae species had similar percentages of extractives when extracted with ethanol: benzene and ethanol. However, hot water extractives were low except for *A. convallis* (Table 3). Compared with the literature on other *Agave* species (Table 9), the extractive percentages in water were similar to the values reported here. *A. tequilana*, *A. angustifolia*, and *A. salmiana* have values between 4.4%–6.0% (Table 9). On the contrary, the values reported in *Agave* for the percentages of extractives in ethanol: benzene and ethanol (Table 9) were low (1.5%–4.0% in ethanol: benzene and 1.3%–5.0% in ethanol) compared to the values reported here (Table 3). For the genera *Beaucarnea*, *Furcraea*, and *Nolina*, there are no reports of extractive percentages in their stems or leaves. In the *Yucca* genus, the literature report that *Y. gloriosa* presents a percentage of total extractives of 1.1 [31], which is low compared to the percentages obtained here (Table 3).

Although extractives in ethanol: benzene and in ethanol are hardly reported in the literature for the species of the genera analyzed here, they have been reported for other succulent species such as cacti [20,21], which had lower percentages of ethanol: benzene (2.5%–4.2%), similar in ethanol (1.0%–9.1%), higher in hot water (8.2%–44.5%) and total extractives (16.7–49.2 %).

In the percentages of lignocellulosic compounds, Table 4 shows that there was heterogeneity in the results within the same genus. In the species that are considered arborescent, it was obtained that the percentages of lignin were low. However, the percentage of cellulose was higher (37.3%–52.2%) and in herbaceous species was lower (31.6%–37.1%). In the hemicelluloses, there is homogeneity between the agaves (20.9%–27.1%), while in the *Yucca* genus, notable differences are observed between *Y. gigantea* (5.7%) concerning the other two species of *Yucca* (21.0% and 30.7%). The differences possibly were due to the type of environment in which they live; *Y. gigantea* is distributed in regions with higher humidity [32], while *Y. filifera* [33,34] and *Y. periculosa* [35] grow in arid zones and semi-desert, respectively. In celluloses, the percentages reported in the literature (Table 9) were high compared to those obtained here (Table 4), possibly due to the differences in the species or the conditions in which they have been developed [36,37].

When comparing the results obtained with succulent species such as cacti, it was observed that the percentages of lignocellulose, in general, are higher in agave species than in non-fibrous wood cacti species [20], while in fibrous species, the percentages were similar [38].

**Table 9.** Percentages of extractives and lignocellulosic compounds of *Agave*, *Furcraea*, and *Yucca*.

Species	S *	Ce	He	Li	TE	W	E–B	Et	Ref
<i>A. angustifolia</i>	L	33.2–44.3	2.6–3.5	2.1–2.9	—	—	—	—	[9]
<i>A. lechuguilla</i>									
<i>A. salmiana</i>									
<i>A. tequilana</i>									
<i>A. americana</i>	L	68.4	15.7	4.9	—	—	—	—	[39]
<i>A. americana</i>	St	65.0	32.0	3.0	—	—	—	—	[40]
<i>A. angustifolia</i>	F	55.0	34.1	20.7	5.3	4.4	1.5	—	[8]
<i>A. angustifolia</i>	F	67.0	25.2	6.3	—	—	—	—	[41]
<i>A. angustifolia</i>	F	64.0	25.0	6.5	2.5	—	—	—	[42]
<i>A. lechuguilla</i>	St	17.7	17.5	7.3	45.3	—	—	—	[43]
<i>A. lechuguilla</i>	St	—	—	9.1	25.7	—	—	—	[44]

Table 9. Cont.

Species	S *	Ce	He	Li	TE	W	E–B	Et	Ref
<i>A. lechuguilla</i>	L	79.8	3–6	15.3	—	—	—	—	[45]
<i>A. fourcroudes</i>		77.6	5.0–7.0	13.1					
<i>A. salmiana</i>	F	48.9	—	8.5	—	—	—	—	[46]
<i>A. salmiana</i>	B	47.3	12.8	4.9	—	—	—	—	[47]
<i>A. salmiana</i>	L St	39.7–45.0	—	7.3–11.9	—	6.0–15.1	—	1.3–3.2	[48]
<i>A. americana</i>									
<i>A. tequilana</i>	L St	—	—	9.8	—	—	—	—	[49]
<i>A. salmiana</i>				11.9					
<i>A. tequilana</i>				8.2					
<i>A. americana</i>	—	43.0	32.0	15.0	—	—	—	—	[50]
<i>A. sisalana</i>	F	49.4	—	21.1	—	10.6	2.9	—	[51]
<i>A. tequilana</i>	F	41.9	—	7.2	—	5.8	3.1	—	[52]
<i>A. tequilana</i>	L St	40.0 and 51.0	—	—	—	—	—	—	[53]
<i>A. tequilana</i>	B	56.0–69.0	—	—	—	—	—	—	[54]
<i>A. tequilana</i>	B	40.9	—	—	—	—	—	—	[55]
<i>A. tequilana</i>	B	42.0	18.5	14.0	—	—	—	—	[56]
<i>A. tequilana</i>	B	—	—	—	—	—	—	—	[57]
<i>A. tequilana</i>	B	44.5	20.1	25.3	—	3.7	3.6	—	[58]
<i>A. tequilana</i>	L	24.7–33.5	10.7–15.2	15.6–19.5	—	—	—	—	[59]
<i>A. tequilana</i>	L	47.0	16.0	9.0	—	—	—	—	[6]
<i>A. americana</i>		50.0	22.0	13.0					
<i>A. lechuguilla</i>	L	46.0–48.0	30.0	11.0	—	4.0	4.0	5.0	[60]
<i>Agave spp.</i>	B	70.0–80.0	5.0–10.0	15.0–20.0	—	—	—	—	[61]
<i>Furcraea foetida</i>	F	68.4	11.5	12.3	—	—	—	—	[62]
<i>Yucca aloifolia</i>	L	52.5	20.5	20.0	—	—	—	—	[63]
<i>Yucca gloriosa</i>	F	66.4	17.5	6.7	1.1	—	—	—	[31]

S: sample; Ce: cellulose, He: hemicellulose, Li: lignin, TE: total extractives, W: hot water extractives, E–B: ethanol–benzene extractives, Et: ethanol, Ref: references. \* B: Bagasse, F: Fiber, L: Leaf, St: Stem.

The differences in the extractive and lignocellulosic compounds between species allowed us to identify four groups through the principal component analysis. The first group with *N. excelsa* and *Y. periculosa* presented a lower amount of hot water and total extractives. This could have implications for their use because various authors consider the hot water and total extractives to represent the nonstructural sugars that are used in fermentation processes for the production of ethanol [8,48,51]. However, in the case of *N. excelsa*, the percentage of cellulose presented in the stem would allow it to be used to obtain cellulosic products (Table 4). The characteristic that distinguishes *Y. filifera* from the other species studied was the presence of a large amount of hemicellulose. This hemicellulose can be transformed into usable sugars either through enzymatic hydrolysis processes or with temperature [9], in addition to the fact that *Y. filifera* presented lower percentages of lignin so that the purification of cellulose would be more efficient [64]. The main characteristic of *Y. gigantea* was the lower amount of hemicelluloses; however, it had a high percentage of cellulose that could be used to obtain cellulosic fibers. The three species of *Yucca* studied here revealed the higher differences in the extractives and lignocellulosic compounds between them, and other species of *Yucca* should be studied in the future to support these findings. All agave species plus *Beaucarnea* and *Furcraea* were grouped together by similar values in the extractive compounds (Table 4). In the lignocellulosic components, the agaves had low percentages of cellulose and lignin; however, they had a higher percentage of hemicelluloses. Finally, chromatographic analyzes can be carried out on all the extractives compounds to identify components with potential use, such as flavonoids and triterpenes, which have the antioxidant capacity and can be used mainly in the food and cosmetic industries [65]. In addition, lignocellulose can be treated in different



ways to obtain various derivatives, as mentioned by Palomo-Briones et al. [66] for *Agave tequilana*: through the elimination of lignin by alkaline, organosolv or enzymatic methods, lignin can be solubilized and fermented to obtain ethanolic derivatives. Hemicelluloses and celluloses can be degraded by acids or enzymes to obtain insoluble fractions and use microcrystalline and nanocrystalline cellulose, while the solubilized carbohydrates can be used in the fermentation to obtain ethanol. Solubilized carbohydrates can also be fermented by anaerobic digestion or dark fermentation to obtain biogas and  $H_2$  which can be used to obtain energy [66]. Therefore, the species analyzed in this work could be used in different ways, both energetically and in the production of paper or cellulose components [21].

#### 4.2. Cellulose Crystallinity

The crystallinity indexes allowed identifying the species that had the highest proportion of crystalline cellulose. The purity of the cellulose could affect these indexes by presenting hemicellulose or lignin residues that alter the peaks [67]. The FTIR spectra can determine the purity of the samples and calculate the proportion of crystalline cellulose [68,69] by the absence of peaks belonging to hemicelluloses [70] and lignin [71].

The most commonly used indexes in conjunction with FTIR are TCI, LOI, and HBI [68,72]. The TCI index provides information about the amount of crystalline or amorphous cellulose in a sample. The peak indicating the presence of crystalline cellulose is  $1370\text{ cm}^{-1}$ , while the peak of  $2900\text{ cm}^{-1}$  [27] indicates the presence of amorphous cellulose. Therefore, if the value of the ratio is greater than one, there will be a greater amount of crystalline cellulose [28]. The LOI index is related to the order of crystalline cellulose, in addition to the fact that the  $1430\text{ cm}^{-1}$  peak shows the presence of crystalline cellulose of type I and the peak  $893\text{ cm}^{-1}$  the presence of type II crystalline cellulose and cellulose amorphous [73]. The order of the crystalline cellulose and LOI peaks can be altered by the type of chemical extraction, and the type of purification used [74]. The HBI index reflects the crystallinity of the sample and its water absorption. Low values reflect a greater amount of crystalline cellulose, while high values indicate the presence of cellulose II or amorphous [27], however, TCI and HBI values are related in terms of cellulose structure and stability, so if they are similar, the cellulose structure has greater stability [28].

Generally, the samples had a higher proportion of crystalline cellulose; however, the type of extraction modifies the order of the cellulose, so the low LOI values reflect the presence of type II crystalline cellulose [75], in addition to possibly the presence of NaOH during purification and the temperature used would alter the order of the crystalline [73]. Furthermore, LOI is correlated with the overall degree of cellulose order, while TCI is directly proportional to the percentage of crystalline cellulose [28]. The similar values of HBI with TCI confirm that the highest proportion of crystalline cellulose predominates among the Asparagaceae species, except the species *A. striata*, *B. gracilis*, and *Y. periculosa*, which had lower crystalline cellulose, and this is reflected in the LOI values that were also the highest [76].

The presence of a greater amount of crystalline cellulose (between 50 and 56% so that the proportion of TCI is 1 to 1.27) in most of the Asparagaceae species agrees with that reported for stems (Table 10). Furthermore, the percentages were also similar for other structures such as fibers in *Agave* (50.07 [46]), *Furcraea* (52.6% [62]), and *Yucca* spp. (55–56% [77]). The other structures have a higher percentage, possibly due to the species analyzed, the type of sample, such as bagasse that no longer has extractives, and some structural sugars, such as hemicelluloses. However, in future studies, X-ray diffraction analysis [78] could be used to confirm the proportion of crystalline cellulose in samples of Asparagaceae species.

**Table 10.** Crystalline index *Agave*, *Furcraea*, and *Yucca*.

Species	Sample	Crystalline Index	Reference
<i>A. salmiana</i>	Fiber	50.07	[46]
<i>A. tequilana</i>	Bagasse	63–68	[54]
<i>A. salmiana</i>	Leaf and stem	45–55	[48]
<i>A. americana</i>			
<i>A. tequilana</i>			
<i>A. tequilana</i>	Bagasse	71	[57]
<i>A. tequilana</i>	Bagasse	60.5	[58]
<i>A. americana</i>	Stem	50.1–64.1	[40]
<i>Yucca</i> spp.	Leaf	76	[77]
<i>Yucca aloifolia</i>	Leaf	69.43	[63]
<i>Yucca</i> spp.	Fiber	55–56	[79]
<i>Furcraea foetida</i>	Fiber	52.6	[62]

#### 4.3. Lignin S/G Ratio

The proportion of S/G obtained for the 10 species reflected that most of the species presented high percentages of syringyl monomers, except for *A. attenuata* (36.9%) and *A. convallis* (48%). The species with the highest percentage was of the *Yucca* genus since it had percentages of 73.9 to 79.5%. The presence of higher percentages of syringyl in species with stem potential allows the purification of cellulose and the degradation of lignin by hydrolytic processes to be more efficient [80] by presenting more bonds of the  $\beta$ -O-4 type and being less condensed [81]. In species with higher percentages of guaiacyl, the stem tissue is hard, and the lignin is difficult to degrade, which is why it is called recalcitrant lignin [82].

Therefore, in the *Yucca* species and generally in the other species of *Agave*, *Beaucarnea*, *Furcraea*, and *Nolina*, by presenting a higher percentage of syringyl, the hydrolyzation process with Kraft would be more efficient [83]. In the literature, there are few reports on the proportion of S/G for *A. fourcroydes*, proportions are reported in fibers (1.05) and spines (1.2) [84], in leaves of *A. sisalana* (2.0) [85], and leaf fibers (3.0–3.5) [86]. In stems, S/G values have been reported for *A. americana* (1.27), *A. angustifolia* (1.29), *A. fourcroydes* (1.40), *A. salmiana* (1.33) y *A. tequilana* (1.57) in untreated samples [11], while for *A. tequilana* S/G values of 4.3 have also been reported in untreated samples [87] while in *A. sisalana* the proportion of S/G in stem fibers is 3.6 [88]. In the other genera analyzed here, there are no reports on the composition of lignin. In general, it is observed that the values obtained are similar to those reported by the aforementioned authors.

The presence of high percentages of syringyl in lignin has also been reported in various fibrous species where it provides resistance to and cellular support [89–91]. However, in succulent species such as cacti, the presence of syringyl monomers is more associated with tissues with non-lignified parenchyma and not fibers [38,92,93], so the presence of syringyl could be associated with a defense mechanism against pathogens [93] as it has been reported for bryophytes, conifers and angiosperms [94–98].

#### 4.4. Cellulose and Lignin Anatomical Distribution

Analyzing the anatomical distribution of lignin and cellulose in the vascular bundles of Asparagaceae species was useful in identifying the location of the main structural components, in addition to explaining the results obtained both in the percentages of lignocellulosic components and in the proportion of S/G [49,99].

In Figure 4, the fluorescence emitted by the tracheary elements, the fibers, and the non-lignified and lignified parenchyma showed that lignin had different emissions in its fluorescence since it ranged from bluish tones to yellow tones. In the species of *A. attenuata* and *A. convallis*, the presence of yellow tones was observed, which would be related to the type of lignin present in the lignified walls. As proposed by Maceda et al. [93], based on a tone scale, yellow to green tones would reflect the presence of guaiacyl-type lignin, while syringyl-type lignin would have shades of lime-green to blue. The difference in the



tones in the emission of fluorescence has already been reported for various species with similar tones [100]. The presence of blue tones in fibers in species with S/G ratios above two [93], as for *Ferocactus hamatacanthus* and *F. pilosus*, whose S/G ratio is 11.7 and 3.5, respectively [38]. Therefore, in the species of Yuccas, whose proportion ranges from 2.8 to 3.9, the presence of fibers and tissue in blue tones responds to the presence of lignin of the syringyl type.

The presence of lignified parenchyma in the stems of the *Yucca* species (Figure 4c–f) agrees with the lignin percentages shown in Table 4 since these species, except for *B. gracilis*, had high lignin values, in contrast to the species of *A. convallis* and *A. attenuata* (Figure 4a,b). Therefore, the presence of lignin is a structural support factor for species of tall size and arborescent shape. However, these species also had high percentages of cellulose (Table 4), with a predominance of crystalline cellulose (Table 7). Cellulose and lignin not only provide structural rigidity but also the proportion of S/G, and the presence of crystalline cellulose could improve water conduction in tracheary elements [101] in addition to protecting against pathogens [91,102]. The species analyzed in this study are naturally distributed in Mexico and *Y. guatemalensis* in Mexico and Guatemala, so it would be interesting to expand the number of genera to determine if there is heterogeneity in a greater number of species of the same genus or if they present homogeneity in the composition of cellulose and lignin.

## 5. Conclusions

The presence of high percentages of cellulose, the predominance of syringyl-type lignin, percentages above 10% of total extractive components, and the high percentages of holocellulose (structural sugars) show that Asparagaceae species have potential in the use of both productions as biofuels as in the production of paper. In addition, the chemical composition that Asparagaceae species present would be related to biological implications such as conduction, support, and protection against pathogens.

**Author Contributions:** Conceptualization, A.M. and T.T.; methodology, A.M., M.S.-H. and T.T.; validation, A.M. and T.T.; investigation, A.M. and T.T.; resources, T.T.; writing—review and editing, A.M., T.T. and M.S.-H. All authors have read and agreed to the published version of the manuscript.

**Funding:** Funding was provided by DGAPA–UNAM postdoctoral fellowship (document number: CJ IC/CTIC I5007I202I) to AM.

**Data Availability Statement:** Raw data and FTIR spectra are available in the Figshare repository: <https://doi.org/10.6084/m9.figshare.21259230.v1> [https://figshare.com/articles/dataset/Chemical-anatomical\\_characterization\\_of\\_stems\\_of\\_Asparagaceae\\_species\\_with\\_potential\\_use\\_for\\_lignocellulosic\\_fibers\\_and\\_biofu-els/21259230](https://figshare.com/articles/dataset/Chemical-anatomical_characterization_of_stems_of_Asparagaceae_species_with_potential_use_for_lignocellulosic_fibers_and_biofu-els/21259230) (accessed on 3 November 2022)

**Acknowledgments:** The authors thank Abisai Josué García for providing the plants from the Botanic Garden, UNAM; thanks to Rubén San Miguel—Chávez for allowing us to use the FTIR in COLPOS. Thanks to Elizabeth Navarro Cerón for allowing us to use the laboratory LANISAF, thanks to Pedro Mercado Ruaro from Laboratorio de Morfo—Anatomía y Citogenética (LANABIO, UNAM), and thanks to Steffany Aguilar Moreno for the support and the laboratory glassware provided.

**Conflicts of Interest:** The authors declare no conflict of interest.

## References

1. Delgado-Lemus, A.; Casas, A.; Téllez, O. Distribution, abundance and traditional management of *Agave potatorum* in the Tehuacán Valley, Mexico: Bases for sustainable use of non-timber forest products. *J. Ethnobiol. Ethnomed.* **2014**, *10*, 63. [CrossRef] [PubMed]
2. Martínez Jiménez, R.; Ruiz-Vega, J.; Caballero Caballero, M.; Silva Rivera, M.E.; Montes Bernabé, J.L. Agaves silvestres y cultivados empleados en la elaboración de mezcal en Sola de vega, Oaxaca, México. *Trop. Subtrop. Agroecosyst.* **2019**, *22*, 477–485.
3. García-Mendoza, A.J.; Franco Martínez, I.S.; Sandoval Gutiérrez, D. Cuatro especies nuevas de *Agave* (Asparagaceae, Agavoideae) del sur de México. *Acta Bot. Mex.* **2019**, *126*, e1461. [CrossRef]
4. Seberg, O.; Petersen, G.; Davis, J.I.; Chris Pires, J.; Stevenson, D.W.; Chase, M.W.; Fay, M.F.; Devey, D.S.; Jørgensen, T.; Sytsma, K.J.; et al. Phylogeny of the Asparagales based on three plastid and two mitochondrial genes. *Am. J. Bot.* **2012**, *99*, 875–889. [CrossRef]
5. Pérez Hernández, E.; Del Carmen Chávez Parga, M.; González Hernández, J.C. Revisión del agave y el mezcal. *Rev. Colomb. Biotecnol.* **2016**, *18*, 148–164. [CrossRef]

6. Corbin, K.R.; Byrt, C.S.; Bauer, S.; Debolt, S.; Chambers, D.; Holtum, J.A.M.; Karem, G.; Henderson, M.; Lahnstein, J.; Beahan, C.T.; et al. Prospecting for energy-rich renewable raw materials: *Agave* leaf case study. *PLoS ONE* **2015**, *10*, e0135382. [\[CrossRef\]](#)
7. Flores-Gómez, C.A.; Escamilla Silva, E.M.; Zhong, C.; Dale, B.E.; Da Costa Sousa, L.; Balan, V. Conversion of lignocellulosic agave residues into liquid biofuels using an AFEX<sup>TM</sup>-based biorefinery. *Biotechnol. Biofuels* **2018**, *11*, 1–18. [\[CrossRef\]](#)
8. Hidalgo-Reyes, M.; Caballero-Caballero, M.; Hernández-Gómez, L.H.; Urriolagoitia-Calderón, G. Chemical and morphological characterization of *Agave angustifolia* bagasse fibers. *Bot. Sci.* **2015**, *93*, 807–817. [\[CrossRef\]](#)
9. Jiménez-Muñoz, E.; Prieto-García, F.; Prieto-Méndez, J.; Acevedo-Sandoval, O.A.; Rodríguez-Laguna, R. Physicochemical characterization of four species of agaves with potential in obtaining pulp for paper making. *DYNA* **2016**, *83*, 232–242. [\[CrossRef\]](#)
10. Davis, S.C.; Dohleman, F.G.; Long, S.P. The global potential for *Agave* as a biofuel feedstock. *GCB Bioenergy* **2011**, *3*, 68–78. [\[CrossRef\]](#)
11. Pérez-Pimienta, J.A.; Mojica-Álvarez, R.M.; Sánchez-Herrera, L.M.; Mittal, A.; Sykes, R.W. Recalcitrance assessment of the agro-industrial residues from five *Agave* species: Ionic liquid pretreatment, saccharification and structural characterization. *BioEnergy Res.* **2018**, *11*, 551–561. [\[CrossRef\]](#)
12. Hill, J.; Nelson, E.; Tilman, D.; Polasky, S.; Tiffany, D. Environmental, economic, and energetic costs and benefits of biodiesel and ethanol biofuels. *Proc. Natl. Acad. Sci. USA* **2006**, *103*, 11206–11210. [\[CrossRef\]](#) [\[PubMed\]](#)
13. Sims, R.E.H.; Mabee, W.; Saddler, J.N.; Taylor, M. An overview of second generation biofuel technologies. *Bioresour. Technol.* **2010**, *1570*–1580. [\[CrossRef\]](#) [\[PubMed\]](#)
14. Comparetti, A.; Febo, P.; Greco, C.; Mammano, M.M.; Orlando, S. Potential production of biogas from prickly pear (*Opuntia ficus-indica* L.) in Sicilian uncultivated areas. *Chem. Eng. Trans.* **2017**, *58*, 559–564. [\[CrossRef\]](#)
15. Gilman, I.S.; Edwards, E.J. Crassulacean acid metabolism. *Curr. Biol.* **2019**, *30*, 51–63. [\[CrossRef\]](#)
16. López Collado, C.J.; Vázquez, A.M.; López-Collado, J.; García-Pérez, E.; Sánchez, Á.S. Crecimiento de *Opuntia ficus-indica* (L.) Mill. en la zona central de Veracruz. *Rev. Mex. Cienc. Agríc.* **2013**, *4*, 1005–1014. [\[CrossRef\]](#)
17. Garbanzo-León, G.; Chavarría-Pérez, G.; Vega-Villalobos, E.V. Correlaciones alométricas en *Hylocereus costaricensis* y *H. monacanthus* (pitahaya): Una herramienta para cuantificar el crecimiento. *Agron. Mesoam.* **2019**, *30*, 425–436. [\[CrossRef\]](#)
18. Loza-Cornejo, S.; Terrazas, T.; López-Mata, L.; Trejo, C. Características morfo-anatómicas y metabolismo fotosintético en plántulas de *Stenocereus queretaroensis* (Cactaceae): Su significado adaptativo. *Interciencia* **2003**, *28*, 83–89.
19. Zúñiga-Estrada, L.; Rosales Robles, E.; Yáñez-Morales, M.d.J.; Jacques-Hernández, C. Características y productividad de una planta MAC, *Agave tequilana* desarrollada con fertigación en Tamaulipas, México. *Rev. Mex. Cienc. Agríc.* **2018**, *9*, 553–564.
20. Maceda, A.; Soto-Hernández, M.; Peña-Valdivia, C.B.; Terrazas, T. Chemical composition of cacti wood and comparison with the wood of other taxonomic groups. *Chem. Biodivers.* **2018**, *15*, e1700574. [\[CrossRef\]](#)
21. Maceda, A.; Soto-Hernández, M.; Peña-Valdivia, C.B.; Trejo, C.; Terrazas, T. Characterization of lignocellulose of *Opuntia* (Cactaceae) species using FTIR spectroscopy: Possible candidates for renewable raw material. *Biomass Convers. Biorefin.* **2020**. [\[CrossRef\]](#)
22. Li, R.; Yang, G.; Chen, J.; He, M. The characterization of hemicellulose extract from corn stalk with stepwise alkali extraction. *Palpu Chongi Gisul/J. Korea Tech. Assoc. Pulp Pap. Ind.* **2017**, *49*, 29–40. [\[CrossRef\]](#)
23. Popescu, C.-M.; Popa, V.I. Analytical methods for lignin characterization. II. Spectroscopic studies. *Cellul. Chem. Technol.* **2006**, *40*, 597–621.
24. Pandey, K.K. Study of the effect of photo-irradiation on the surface chemistry of wood. *Polym. Degrad. Stab.* **2005**, *90*, 9–20. [\[CrossRef\]](#)
25. Nelson, M.L.; O'Connor, R.T. Relation of certain infrared bands to cellulose crystallinity and crystal latticed type. Part I. Spectra of lattice types I, II, III and of amorphous cellulose. *J. Appl. Polym. Sci.* **1964**, *8*, 1311–1324. [\[CrossRef\]](#)
26. Ciolacu, D.; Ciolacu, F.; Popa, V.I. Amorphous cellulose—structure and characterization. *Cellul. Chem. Technol.* **2011**, *45*, 13–21.
27. Poletto, M.; Ornaghi, H.L.; Zattera, A.J. Native cellulose: Structure, characterization and thermal properties. *Materials* **2014**, *7*, 6105–6119. [\[CrossRef\]](#)
28. Cichosz, S.; Masek, A. IR study on cellulose with the varied moisture contents: Insight into the supramolecular structure. *Materials* **2020**, *13*, 4573. [\[CrossRef\]](#)
29. Arias, S.; Terrazas, T. Variación en la anatomía de la madera de *Pachycereus pecten-aboriginum* (Cactaceae). *An. Inst. Biol. Univ. Nac. Autón. Méx.* **2001**, *72*, 157–169.
30. Nakaba, S.; Kitin, P.; Yamagishi, Y.; Begum, S.; Kudo, K.; Nugroho, W.D.; Funada, R. Three-dimensional imaging of cambium and secondary xylem cells by confocal laser scanning microscopy. *Plant Microtech. Protoc.* **2015**, 431–465. [\[CrossRef\]](#)
31. Taban, E.; Mirzaei, R.; Faridan, M.; Samaei, E.; Salimi, F.; Tajpoor, A.; Ghalenoei, M. Morphological, acoustical, mechanical and thermal properties of sustainable green *Yucca* (*Y. gloriosa*) fibers: An exploratory investigation. *J. Environ. Health Sci. Eng.* **2020**, *18*, 883–896. [\[CrossRef\]](#)
32. Nataren-Velazquez, J.; Del Angel-Pérez, A.L.; Megchún-García, J.V.; Ramírez-Herrera, E.; Ibarra-Pérez, F. Colecta y caracterización morfológica de izote (*Yucca elephantipes*) y cruceta (*Acanthocereus tetragonus*), del estado de Veracruz. In *Prospectiva, de la Investigación Agrícola en el Siglo XXI en México*; Avendaño Ruiz, B.D., Bautista Ortega, J., Del Angel-Pérez, A.L., Ireta Paredes, A.d.R., Martínez-Trejo, G., Pérez Hernández, P., Schwentesius Ridemann, R., Eds.; Universidad Autónoma de Chapingo and Plaza y Valdés, S.L.: Texcoco, México, 2020; pp. 137–149.

33. Mora-Olivo, A.; Hurtado-González, M.; Gaona-García, G.; Treviño-Carreón, J. Las flores comestibles del desierto. *CienciaUAT* **2009**, *4*, 10–13.
34. Granados-Sánchez, D.; Sánchez-González, A.; Granados-Victorino, R.L.; de la Rosa, A.B. Ecología de la vegetación del desierto chihuahuense. *Rev. Chapingo Ser. Cienc. For. Y Ambient.* **2011**, *18*, 111–130. [\[CrossRef\]](#)
35. Hernández-Moreno, M.M.; Téllez-Valdés, O.; Martínez-Meyer, E.; Islas-Saldaña, L.A.; Salazar-Rojas, V.M.; Macías-Cuéllar, H. Distribución de la cobertura vegetal y del uso del terreno del municipio de Zapotitlán, Puebla, México. *Rev. Mex. Biodivers.* **2021**, *92*, e923649. [\[CrossRef\]](#)
36. Moura, J.C.M.S.; Bonine, C.A.V.; de Oliveira Fernandes Viana, J.; Dornelas, M.C.; Mazzafera, P. Abiotic and biotic stresses and changes in the lignin content and composition in plants. *J. Integr. Plant Biol.* **2010**, *52*, 360–376. [\[CrossRef\]](#) [\[PubMed\]](#)
37. Lipiec, J.; Doussan, C.; Nosalewicz, A.; Kondracka, K. Effect of drought and heat stresses on plant growth and yield: A review. *Int. Agrophys.* **2013**, *27*, 463–477. [\[CrossRef\]](#)
38. Reyes-Rivera, J.; Canché-Escamilla, G.; Soto-Hernández, M.; Terrazas, T. Wood chemical composition in species of Cactaceae the relationship between lignification and stem morphology. *PLoS ONE* **2015**, *10*, e0123919. [\[CrossRef\]](#)
39. Mysamy, K.; Rajendran, I. Investigation on physio-chemical and mechanical properties of raw and alkali-treated *Agave americana* fiber. *J. Reinf. Plast. Compos.* **2010**, *29*, 2925–2935. [\[CrossRef\]](#)
40. Krishnadev, P.; Subramanian, K.S.; Janavi, G.J.; Ganapathy, S.; Lakshmanan, A. Synthesis and characterization of nano-fibrillated cellulose derived from green *Agave americana* L. Fiber. *BioResources* **2020**, *15*, 2442–2458. [\[CrossRef\]](#)
41. Rosli, N.A.; Ahmad, I.; Abdullah, I. Isolation and characterization of cellulose nanocrystals from *Agave angustifolia* fibre. *BioResources* **2013**, *8*, 1893–1908. [\[CrossRef\]](#)
42. Teli, M.D.; Jadhav, A.C. Effect of alkali treatment on the properties of *Agave angustifolia* v. *marginata* fibre. *Int. Res. J. Eng. Technol.* **2016**, *3*, 2754–2761.
43. Carmona, J.E.; Morales-Martínez, T.K.; Mussatto, S.I.; Castillo-Quiroz, D.; Ríos-González, L.J. Chemical, structural and functional properties of lechuguilla (*Agave lechuguilla* Torr.). *Rev. Mex. Cienc. For.* **2017**, *8*, 100–122.
44. Ortiz-Méndez, O.H.; Morales-Martínez, T.K.; Ríos-González, L.J.; Rodríguez-De La Garza, J.A.; Quintero, J.; Aroca, G. Bioethanol production from *Agave lechuguilla* biomass pretreated by autohydrolysis. *Rev. Mex. Ing. Quím.* **2017**, *16*, 467–476.
45. Vieira, M.C.; Heinze, T.; Antonio-Cruz, R.; Mendoza-Martínez, A.M. Cellulose derivatives from cellulosic material isolated from *Agave lechuguilla* and *A. fourcroydes*. *Cellulose* **2002**, *9*, 203–212. [\[CrossRef\]](#)
46. De Dios Naranjo, C.; Alamilla-Beltrán, L.; Gutiérrez-Lopez, G.F.; Terres-Rojas, E.; Solorza-Feria, J.; Romero-Vargas, S.; Yee-Madeira, H.T.; Areli, F.-M.; Mora-Escobedo, R. Aislamiento y caracterización de celulosas obtenidas de fibras de *Agave salmiana* aplicando dos métodos de extracción ácido-alcali. *Rev. Mex. Cienc. Agríc.* **2016**, *7*, 31–43.
47. Bernardo, G.R.R.; Rene, R.M.J. Contribution of agro-waste material main components (hemicelluloses, cellulose, and lignin) to the removal of chromium (III) from aqueous solution. *J. Chem. Technol. Biotechnol.* **2009**, *84*, 1533–1538. [\[CrossRef\]](#)
48. Li, H.; Foston, M.B.; Kumar, R.; Samuel, R.; Gao, X.; Hu, F.; Ragauskas Cd, A.J.; Wyman, C.E. Chemical composition and characterization of cellulose for Agave as a fast-growing, drought-tolerant biofuels feedstock. *RSC Adv.* **2012**, *2*, 4951–4958. [\[CrossRef\]](#)
49. Li, H.; Pattathil, S.; Foston, M.B.; Ding, S.Y.; Kumar, R.; Gao, X.; Mittal, A.; Yarbrough, J.M.; Himmel, M.E.; Ragauskas, A.J.; et al. *Agave* proves to be a low recalcitrant lignocellulosic feedstock for biofuels production on semi-arid lands. *Biotechnol. Biofuels* **2014**, *7*, 50. [\[CrossRef\]](#)
50. McDougall, G.J.; Morrison, I.M.; Stewart, D.; Weyers, J.D.B.; Hillman, J.R. Plant fibres: Botany, chemistry and processing for industrial use. *J. Sci. Food Agric.* **1993**, *62*, 1–20. [\[CrossRef\]](#)
51. Kestur G., S.; Flores-Sahagun, T.H.S.; Dos Santos, L.P.; Dos Santos, J.; Mazzaro, I.; Mikowski, A. Characterization of blue agave bagasse fibers of Mexico. *Compos. Part A Appl. Sci. Manuf.* **2013**, *45*, 153–161. [\[CrossRef\]](#)
52. Iñiguez, G.; Acosta, N.; Martínez, L.; Parra, J.; González, O. Utilización de supproductos de la industria tequilera. Parte 7. Compostaje de bagazo de agave y vinazas tequileras. *Rev. Int. Contam. Ambient.* **2005**, *21*, 37–50.
53. Robles, E.; Fernández-Rodríguez, J.; Barbosa, A.M.; Gordobil, O.; Carreño, N.L.V.; Labidi, J. Production of cellulose nanoparticles from blue agave waste treated with environmentally friendly processes. *Carbohydr. Polym.* **2018**, *183*, 294–302. [\[CrossRef\]](#) [\[PubMed\]](#)
54. Hernández, J.A.; Romero, V.H.; Escalante, A.; Toriz, G.; Rojas, O.J.; Sulbarán, B.C. *Agave tequilana* bagasse as source of cellulose nanocrystals via organosolv treatment. *BioResources* **2018**, *13*, 3603–3614. [\[CrossRef\]](#)
55. Robles-García, M.Á.; Del-Toro-Sánchez, C.L.; Márquez-Ríos, E.; Barrera-Rodríguez, A.; Aguilar, J.; Aguilar, J.A.; Reynoso-Marín, F.J.; Ceja, I.; Dórame-Miranda, R.; Rodríguez-Félix, F. Nanofibers of cellulose bagasse from *Agave tequilana* Weber var. *azul* by electrospinning: Preparation and characterization. *Carbohydr. Polym.* **2018**, *192*, 69–74. [\[CrossRef\]](#) [\[PubMed\]](#)
56. Ramírez-Cortina, C.; Alonso-Gutiérrez, M.S.; Rigal, L. Tratamiento alcalino de los residuos agroindustriales de la producción del tequila, para su uso como complemento de alimento de rumiantes. *Rev. AIDIS Ing. Y Cienc. Ambient.* **2012**, *5*, 69–77.
57. Espino, E.; Cakir, M.; Domemek, S.; Román-Gutiérrez, A.D.; Belgacem, N.; Bras, J. Isolation and characterization of cellulose nanocrystals from industrial by-products of *Agave tequilana* and barley. *Ind. Crop. Prod.* **2014**, *62*, 552–559. [\[CrossRef\]](#)
58. Palacios Hinestroza, H.; Hernández Diaz, J.A.; Esquivel Alfaro, M.; Toriz, G.; Rojas, O.J.; Sulbarán-Rangel, B.C. Isolation and characterization of nanofibrillar cellulose from *Agave tequilana* Weber bagasse. *Adv. Mater. Sci. Eng.* **2019**, *2019*, 1342547. [\[CrossRef\]](#)

59. Rijal, D.; Walsh, K.B.; Subedi, P.P.; Ashwath, N. Quality estimation of *Agave tequilana* leaf for bioethanol production. *J. Near Infrared Spectrosc.* **2017**, *24*, 453–465. [\[CrossRef\]](#)
60. Márquez, A.; Cazaurang, N.; González, I.; Colunga-GarcíaMarín, P. Extraction of chemical cellulose from the fibers of *Agave lechuguilla* Torr. *Econ. Bot.* **1996**, *50*, 465–468. [\[CrossRef\]](#)
61. Ponce-Reyes, C.E.; Chanona-Pérez, J.J.; Garibay-Febles, V.; Palacios-González, E.; Karamath, J.; Terrés-Rojas, E.; Calderón-Domínguez, G. Preparation of cellulose nanoparticles from agave waste and its morphological and structural characterization. *Rev. Mex. Ing. Quím.* **2014**, *13*, 897–906.
62. Manimaran, P.; Senthamaraiannan, P.; Sanjay, M.R.; Marichelvam, M.K.; Jawaid, M. Study on characterization of *Furcraea foetida* new natural fiber as composite reinforcement for lightweight applications. *Carbohydr. Polym.* **2018**, *181*, 650–658. [\[CrossRef\]](#) [\[PubMed\]](#)
63. do Nascimento, H.M.; dos Santos, A.; Duarte, V.A.; Bittencourt, P.R.S.; Radovanovic, E.; Fávaro, S.L. Characterization of natural cellulosic fibers from *Yucca aloifolia* L. leaf as potential reinforcement of polymer composites. *Cellulose* **2021**, *28*, 5477–5492. [\[CrossRef\]](#)
64. Razali, N.A.M.; Sohaimi, R.M.; Othman, R.N.I.R.; Abdullah, N.; Demon, S.Z.N.; Jasmani, L.; Yunus, W.M.Z.W.; Ya'acob, W.M.H.W.; Salleh, E.M.; Norizan, M.N.; et al. Comparative study on extraction of cellulose fiber from rice straw waste from chemo-mechanical and pulping method. *Polymers* **2022**, *14*, 387. [\[CrossRef\]](#) [\[PubMed\]](#)
65. Álvarez-Chávez, J.; Villamiel, M.; Santos-Zea, L.; Ramírez-Jiménez, A.K. *Agave* by-products: An overview of their nutraceutical value, current applications, and processing methods. *Polysaccharides* **2021**, *2*, 720–743. [\[CrossRef\]](#)
66. Palomo-Briones, R.; López-Gutiérrez, I.; Islas-Lugo, F.; Galindo-Hernández, K.L.; Munguía-Aguilar, D.; Rincón-Pérez, J.A.; Cortés-Carmona, M.A.; Alatríste-Mondragón, F.; Razo-Flores, E. *Agave* bagasse biorefinery: Processing and perspectives. *Clean Technol. Environ. Policy* **2018**, *20*, 1423–1441. [\[CrossRef\]](#)
67. Fuller, M.E.; Andaya, C.; McClay, K. Evaluation of ATR-FTIR for analysis of bacterial cellulose impurities. *J. Microbiol. Methods* **2018**, *144*, 145–151. [\[CrossRef\]](#)
68. Zaltariov, M.-F. FTIR investigation on crystallinity of hydroxypropyl methyl cellulose-based polymeric blends. *Cellul. Chem. Technol. Cellul. Chem. Technol.* **2021**, *55*, 981–988. [\[CrossRef\]](#)
69. Kruer-Zerhusen, N.; Cantero-Tubilla, B.; Wilson, D.B. Characterization of cellulose crystallinity after enzymatic treatment using Fourier transform infrared spectroscopy (FTIR). *Cellulose* **2018**, *25*, 37–48. [\[CrossRef\]](#)
70. Chen, C.J.; Luo, J.J.; Huang, X.P.; Zhao, S.K. Analysis on cellulose crystalline and FTIR spectra of artocarpus heterophyllus Lam wood and its main chemical compositions. *Adv. Mater. Res.* **2011**, *236–238*, 369–375. [\[CrossRef\]](#)
71. Lionetto, F.; Del Sole, R.; Cannoletta, D.; Vasapollo, G.; Maffezzoli, A. Monitoring wood degradation during weathering by cellulose crystallinity. *Materials* **2012**, *5*, 1910–1922. [\[CrossRef\]](#)
72. Poletto, M.; Pistor, V.; Santana, R.M.C.; Zattera, A.J. Materials produced from plant biomass: Part II: Evaluation of crystallinity and degradation kinetics of cellulose. *Mater. Res.* **2012**, *15*, 421–427. [\[CrossRef\]](#)
73. Široký, J.; Blackburn, R.S.; Bechtold, T.; Taylor, J.; White, P. Attenuated total reflectance Fourier-transform Infrared spectroscopy analysis of crystallinity changes in lyocell following continuous treatment with sodium hydroxide. *Cellulose* **2010**, *17*, 103–115. [\[CrossRef\]](#)
74. Hofmann, D.; Fink, H.P.; Philipp, B. Lateral crystallite size and lattice distortions in cellulose II samples of different origin. *Polymer* **1989**, *30*, 237–241. [\[CrossRef\]](#)
75. Kljun, A.; Benians, T.A.S.; Goubet, F.; Meulewaeter, F.; Knox, J.P.; Blackburn, R.S. Comparative analysis of crystallinity changes in cellulose i polymers using ATR-FTIR, X-ray diffraction, and carbohydrate-binding module probes. *Biomacromolecules* **2011**, *12*, 4121–4126. [\[CrossRef\]](#)
76. Colom, X.; Carrillo, F. Crystallinity changes in lyocell and viscose-type fibres by caustic treatment. *Eur. Polym. J.* **2002**, *38*, 2225–2230. [\[CrossRef\]](#)
77. Kamali Moghaddam, M.; Torabi, T. Cellulose microfibers isolated from *Yucca* leaves: Structural, chemical, and thermal properties. *J. Nat. Fibers* **2022**. [\[CrossRef\]](#)
78. Beluns, S.; Gaidukovs, S.; Platnieks, O.; Gaidukova, G.; Mierina, I.; Grase, L.; Starkova, O.; Brazdausks, P.; Thakur, V.K. From wood and hemp biomass wastes to sustainable nanocellulose foams. *Ind. Crop. Prod.* **2021**, *170*, 113780. [\[CrossRef\]](#)
79. Moghaddam, M.K.; Karimi, E. Structural and physical characteristics of the *yucca* fiber. *J. Ind. Text.* **2020**, *51*, 8018S–8034S. [\[CrossRef\]](#)
80. Alves, A.; Simoes, R.; Stackpole, D.J.; Vaillancourt, R.E.; Potts, B.M.; Schwanninger, M.; Rodrigues, J. Determination of the syringyl/guaiacyl ratio of *Eucalyptus globulus* wood lignin by near infrared-based partial least squares regression models using analytical pyrolysis as the reference method. *J. Near Infrared Spectrosc.* **2011**, *19*, 343–348. [\[CrossRef\]](#)
81. Wang, C.; Li, H.; Li, M.; Bian, J.; Sun, R. Revealing the structure and distribution changes of *Eucalyptus* lignin during the hydrothermal and alkaline pretreatments. *Sci. Rep.* **2017**, *7*, 593. [\[CrossRef\]](#)
82. Li, M.; Pu, Y.; Ragauskas, A.J. Current understanding of the correlation of lignin structure with biomass recalcitrance. *Front. Chem.* **2016**, *4*, 45. [\[CrossRef\]](#) [\[PubMed\]](#)
83. Ralph, J.; Landucci, L.L. NMR of Lignins. In *Lignin and Lignans; Advances in Chemistry*; Heitner, C., Dimmel, D.R., Schmidt, J.A., Eds.; Taylor & Francis Group: Boca Raton, FL, USA, 2010; pp. 137–234.



84. Morán-Velázquez, D.C.; Monribot-Villanueva, J.L.; Bourdon, M.; Tang, J.Z.; López-Rosas, I.; Maceda-López, L.F.; Villalpando-Aguilar, J.L.; Rodríguez-López, L.; Gauthier, A.; Trejo, L.; et al. Unravelling chemical composition of agave spines: News from *Agave fourcroydes* Lem. *Plants* **2020**, *9*, 1642. [[CrossRef](#)] [[PubMed](#)]
85. Del Río, J.C.; Rencoret, J.; Marques, G.; Gutiérrez, A.; Ibarra, D.; Santos, J.I.; Jiménez-Barbero, J.; Zhang, L.; Martínez, Á.T. Highly Acylated (acetylated and/or p-coumaroylated) native lignins from diverse herbaceous plants. *J. Agric. Food Chem.* **2008**, *56*, 9525–9534. [[CrossRef](#)] [[PubMed](#)]
86. Del Río, J.C.; Prinsen, P.; Cadena, E.M.; Ngel, A.; Martínez, T.; Gutiérrez, A.; Rencoret, J. Lignin–carbohydrate complexes from sisal (*Agave sisalana*) and abaca (*Musa textilis*): Chemical composition and structural modifications during the isolation process. *Planta* **2016**, *243*, 1143–1158. [[CrossRef](#)]
87. Perez-Pimienta, J.A.; Flores-Gómez, C.A.; Ruiz, H.A.; Sathitsuksanoh, N.; Balan, V.; da Costa Sousa, L.; Dale, B.E.; Singh, S.; Simmons, B.A. Evaluation of *Agave* bagasse recalcitrance using AFEX<sup>TM</sup>, autohydrolysis, and ionic liquid pretreatments. *Bioresour. Technol.* **2016**, *211*, 216–223. [[CrossRef](#)]
88. Rencoret, J.; Marques, G.; Gutiérrez, A.; Ibarra, D.; Li, J.; Gellerstedt, G.; Santos, J.I.; Jiménez-Barbero, J.; Martínez, Á.T.; Del Río, J.C. Structural characterization of milled wood lignins from different eucalypt species. *Holzforschung* **2008**, *62*, 514–526. [[CrossRef](#)]
89. Lee, Y.; Voit, E.O. Mathematical modeling of monolignol biosynthesis in *Populus* xylem. *Math. Biosci.* **2010**, *228*, 78–89. [[CrossRef](#)]
90. Barros, J.; Serk, H.; Granlund, I.; Pesquet, E. The cell biology of lignification in higher plants. *Ann. Bot.* **2015**, *115*, 1053–1074. [[CrossRef](#)]
91. Li, L.; Cheng, X.F.; Leshkevich, J.; Umezawa, T.; Harding, S.A.; Chiang, V.L. The last step of syringyl monolignol biosynthesis in angiosperms is regulated by a novel gene encoding sinapyl alcohol dehydrogenase. *Plant Cell* **2001**, *13*, 1567–1585. [[CrossRef](#)]
92. Reyes-Rivera, J.; Soto-Hernández, M.; Canché-Escamilla, G.; Terrazas, T. Structural characterization of lignin in four cacti wood: Implications of lignification in the growth form and succulence. *Front. Plant Sci.* **2018**, *871*, 1518. [[CrossRef](#)]
93. Maceda, A.; Reyes-Rivera, J.; Soto-Hernández, M.; Terrazas, T. Distribution and chemical composition of lignin in secondary xylem of Cactaceae. *Chem. Biodivers.* **2021**, *18*, e2100431. [[CrossRef](#)] [[PubMed](#)]
94. Weng, J.-K.; Banks, J.A.; Chapple, C. Parallels in lignin biosynthesis: A study in *Selaginella moellendorffii* reveals convergence across 400 million years of evolution. *Commun. Integr. Biol.* **2008**, *1*, 20–22. [[CrossRef](#)] [[PubMed](#)]
95. Weng, J.-K.; Li, X.; Stout, J.; Chapple, C. Independent origins of syringyl lignin in vascular plants. *Proc. Natl. Acad. Sci. USA* **2008**, *105*, 7887–7892. [[CrossRef](#)] [[PubMed](#)]
96. Lange, B.M.; Lapierre, C.; Sandermann, H. Elicitor-induced spruce stress lignin: Structural similarity to early developmental lignins. *Plant Physiol.* **1995**, *108*, 1277–1287. [[CrossRef](#)] [[PubMed](#)]
97. Menden, B.; Kohlhoff, M.; Moerschbacher, B.M. Wheat cells accumulate a syringyl–rich lignin during the hypersensitive resistance response. *Phytochemistry* **2007**, *68*, 513–520. [[CrossRef](#)] [[PubMed](#)]
98. Skyba, O.; Douglas, C.J.; Mansfield, S.D. Syringyl–Rich lignin renders poplars more resistant to degradation by wood decay fungi. *Appl. Environ. Microbiol.* **2013**, *79*, 2560–2571. [[CrossRef](#)]
99. Li, Y.; Mai, Y.W.; Ye, L. Sisal fibre and its composites: A review of recent developments. *Compos. Sci. Technol.* **2000**, *60*, 2037–2055. [[CrossRef](#)]
100. De Micco, V.; Aronne, G. Combined histochemistry and autofluorescence for identifying lignin distribution in cell walls. *Biotech. Histochem.* **2007**, *82*, 209–216. [[CrossRef](#)]
101. Pereira, L.; Domingues-Junior, A.P.; Jansen, S.; Choat, B.; Mazzafera, P. Is embolism resistance in plant xylem associated with quantity and characteristics of lignin? *Trees Struct. Funct.* **2018**, *32*, 349–358. [[CrossRef](#)]
102. Martone, P.T.; Estevez, J.M.; Lu, F.; Ruel, K.; Denny, M.W.; Somerville, C.; Ralph, J. Discovery of lignin in seaweed reveals convergent evolution of cell–wall architecture. *Curr. Biol.* **2009**, *19*, 169–175. [[CrossRef](#)]